

Experimental and Numerical Investigation of Sealing Performance of Turbine Rim Seals

Kenji TERAMACHI¹, Masaaki HAMABE²,
Takashi MANABE² and Nobutaka YANAGIDANI²

¹ Engine Technology Department
Ishikawajima-harima Heavy Industries Co., Ltd.
3-5-1 Mukodai-cho, NishiTokyo-shi, Tokyo 188-8555, JAPAN
Phone: +81-424-60-1341, FAX: +81-424-60-1355, E-mail: kenji_teramachi@ihi.co.jp
² Ishikawajima-harima Heavy Industries Co., Ltd.

ABSTRACT

Performance of turbine rim seals was investigated for the upstream cavity. A rim seal configuration often adopted in actual engines was examined for both with overlap and with gap. Guide vanes (airfoil-shaped) and rotor blades (not airfoil-shaped) were installed to simulate the wake and the upstream potential respectively. CO₂ concentration measurement was carried out for evaluating seal effectiveness. Three-dimensional unsteady CFD analysis was carried out to get information about the flow structure in the rim seal.

It was shown that the presence of rotor blades degraded seal effectiveness whether there is overlap or gap. The effect of fin overlap showed adverse trend between the cases with and without rotor blades. In case with rotor blades, seal effectiveness was higher for the rim seal with gap. It may be related to the mainstream static pressure distribution generated by the interference between blade upstream potential and injected cooling air.

NOMENCLATURE

b	: Outer radius of the cavity
C_w	: Non-dimensional flow coefficient
\dot{m}	: Local mass flux
P	: Static pressure
P_d	: Dynamic pressure
P_m	: Mainstream static pressure
Q	: Volumetric flow rate
r	: Radial coordinate
Re_m	: Mainstream Reynolds number
Re_r	: Rotational Reynolds number
V_{ax}	: Mainstream axial velocity
η	: Seal effectiveness
ν	: Kinematic viscosity
ϕ	: Carbon dioxide concentration
ω	: Angular velocity of rotor disk

Subscripts

M	: Mainstream
C	: Cooling air
min	: Minimum value

INTRODUCTION

As is well-known, mainstream gas ingestion into cavities around turbine disks are observed in aircraft and industrial gas turbine engines. Ingested gas raises the temperature in the cavity, and as a result the temperature of rotating parts such as disks, seals, etc. also rise and have significant damages to their lives. In order to avoid

such kind of risk, secondary air bled off from compressor is supplied to the cavities as "purge air" and rotating and stationary parts (usually platforms of rotor blades and inner bands of nozzle guide vanes) are designed to form a radial or axial clearance seals at rim portion of the cavities. These efforts reduce the amount of mainstream gas ingested into the cavity and keep the temperature in the cavity low enough for rotating parts to meet their required lives. However, as secondary air has a negative impact on engine performance, cavity purge should be accomplished by as little air as possible. Therefore, it is very important to predict the amount of mainstream gas ingested into cavities as accurately as possible.

There are several flow mechanisms that affect mainstream gas ingestion, including disk pumping, circumferential asymmetry of mainstream static pressure and interaction of stator vanes and rotor blades. Many comprehensive investigations have been carried out so far to get a better understanding of this phenomenon.

Early works focused on the disk pumping effect that draws flow inward to the rotor-stator disk cavity to compensate the flow pumped outward in the boundary layer formed on the rotor disk surface. Bayley and Owen (1970) examined a shrouded rotor-stator system with a simple axial gap in a quiescent environment. They established a correlation for the minimum dimensionless cooling flow rate ($C_{w,min}$) required to prevent ingestion. Phadke and Owen (1983) also found a linear relationship between $C_{w,min}$ and the rotational Reynolds number similar to that established by Bayley and Owen.

Several workers have confirmed the influence of mainstream flow, particularly circumferential asymmetry of static pressure on cavity rim sealing. Abe et al. (1979), Dadkhah et al. (1991) and Hamabe and Ishida (1992) carried out experiments to measure mainstream gas ingestion by tracer gas technique. In these experiments, static pressure asymmetry was generated by nozzle guide vanes or other disturbances placed in the mainstream annulus. They agreed on the importance of the presence of mainstream flow.

Chew et al. (1994) performed experiments on mainstream gas ingestion for a stator-rotor system with guide vanes. They varied the axial distance between vane trailing edge and rim seal gap and thus varied the magnitude of circumferential pressure asymmetry. Measured seal effectiveness was found to depend on the magnitude of circumferential pressure asymmetry at the seal gap. They also found that the rotational Reynolds number had little effect on seal effectiveness. Green and Turner (1994) examined mainstream gas ingestion for a stator-rotor system with both stator vanes and rotor blades. They found that the presence of rotor blades improved seal effectiveness. On the other hand, according to Bohn et al. (2000), it

depends on the geometry of rim seal whether the presence of rotor blades improves seal effectiveness or not.

In recent works, the accuracy of CFD analysis has been discussed. Hills et al. (1997) carried out experimental and CFD studies. Comparison of three-dimensional steady CFD solutions with measured pressure showed good agreement at lower purge flow rates while the difference was larger at higher flow rates. This was considered to be due to the complicated interaction of the purge air and mainstream flows that could not be predicted by CFD. Roy et al. (2000) also showed good agreement between steady CFD solutions and measured pressure. Bohn et al. (2000) carried out three-dimensional unsteady CFD analyses for a stator-rotor system with both stator vanes and rotor blades. They found qualitative agreement to a certain degree although there were some differences between CFD solutions and measured levels of ingestion.

This paper presents experimental and numerical investigation results concerning mainstream gas ingestion into the cavity located upstream of the rotor disk in the presence of stator vanes. In order to investigate the effect of the presence of rotor blades, experiments were carried out for both with and without rotor blades. Two types of rim seals of basically same configuration were examined. The difference was whether there was an overlap or a gap between the rotor fin and the stator fin. Operating conditions were systematically varied in the range covering those of actual gas turbine engines. Three-dimensional unsteady CFD analysis was carried out in order to get information about the flow structure in the rim seal area.

A brief description of the test rig and instrumentation as well as numerical analysis procedure is given in the next section. Discussion of the results for both experiments and numerical analyses will follow next. Finally the conclusions from this study are summarized.

This study was carried out as a part of "Research and Development of Environmentally Compatible Propulsion System for New-Generation Supersonic Transport (ESPR) project".

EXPERIMENTAL APPARATUS & PROCEDURE

Test Rig

Cross section of the test rig is shown in Fig.1. Air simulating mainstream is supplied from a gas turbine driven compressor to the annular duct after metered by an orifice. Flow straightener, not shown in this figure, was installed upstream of the test section in order to reduce circumferential deflection of the mainstream. Air simulating cooling air is supplied to the cavity through a tube located at center of the stator disk after metered by an orifice.

Geometry of the cavity is shown in Fig.2. The cavity is formed between the stator disk and the rotor disk driven by an inverter motor. Outer diameter and width of the cavity are 600mm, 20mm respectively.

36 guide vanes were installed in the mainstream around the stator disk. The profile of guide vanes was airfoil-shaped and the exit flow angle was 65 degrees. The position of the trailing edge of guide vanes was 3.5mm upstream of the stator disk surface.

As for the rotor disk, 36 rotor blades were installed. The shape of rotor blades was a simple cylinder of 12.5mm diameter (not airfoil-shaped) to simulate the upstream potential effect, so their diameter was set similar to those of high-pressure turbine first stage rotor blades of actual engines. In addition, these rotor blades were able to be detached from the rotor disk so that the effect of the presence of rotor blades on mainstream gas ingestion could be experimentally investigated.

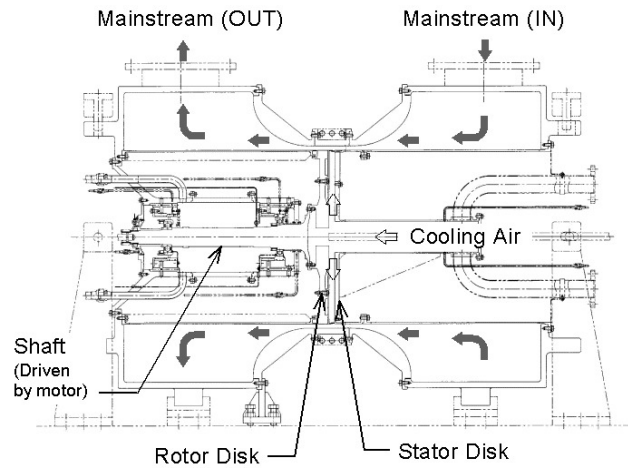


Fig.1 Cross section of test rig

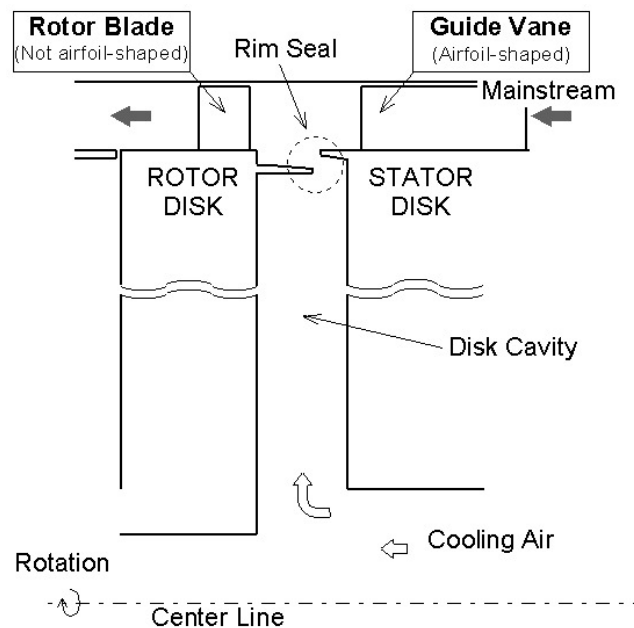


Fig.2 Geometry of the cavity

Rim Seal Configuration

Two types of rim seal shown in Fig.3 were examined. The typical rim seal often adopted for high-pressure turbines of actual engines has an outer fin on the stator (extending downstream from the inner band of the nozzle guide vane) and an inner fin on the rotor (usually extending upstream from the platform of the rotor blade). So the rim seals examined here were designed to have similar configuration. The difference between two types of rim seal is whether there is an overlap or a gap between both fins. There is a certain gap between both fins in case of SEAL-1. Meanwhile there is a certain overlap in case of SEAL-2. For both rim seals the length of the fin on the rotor is kept equal.

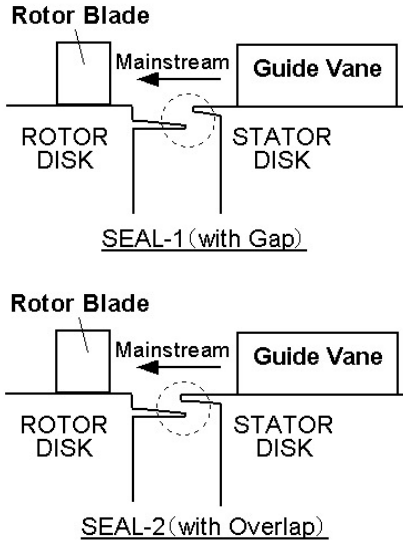


Fig.3 Rim seal configurations

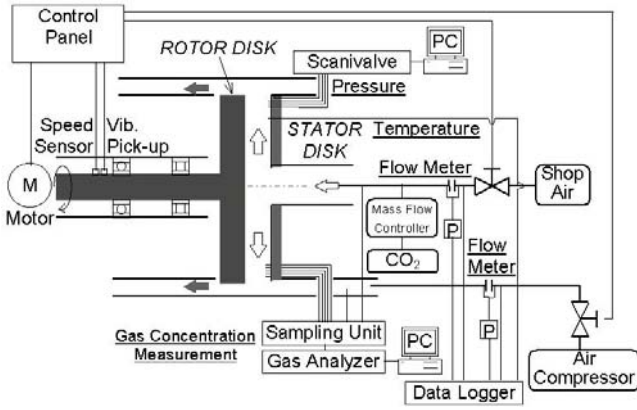


Fig.4 Schematic of test rig

Static Pressure Measurement

Schematic diagram of the test rig is shown in Fig.4.

Static pressure distribution in the cavity was measured by pressure taps on the stator disk surface. Pressure taps are arranged on two pitches of guide vanes at 6 radial positions where r/b ranging from 0.80 to 0.95. Static pressure distribution in the mainstream annulus was also measured by pressure taps located at the same circumferential positions as those in the cavity. Static pressure distribution in the mainstream annulus was also measured at the inlet (upstream of the guide vanes) and the exit (downstream of the rotor blades) of the test section.

All of the static pressures in the cavity and the mainstream were measured by PC-controlled Scanivalves operating in parallel. Pressures at the inlet and outlet of the test section and the orifice differential pressures were measured by individual transducers and recorded on a data logger.

Gas Concentration Measurement

In order to evaluate the amount of mainstream gas ingested into the cavity, tracer gas technique was applied. Carbon dioxide (CO_2) was supplied at constant rate and mixed uniformly with purge air before entering the test rig.

Gas in the cavity was sampled by five axially traversable probes located at five radial positions where r/b ranging from 0.73 to 0.93. Two sets of probes were installed at two circumferential positions relative to the guide vanes i.e., at the same angular position as a vane trailing edge and at the mid-pitch of vane trailing edge.

Seal effectiveness defined by

$$\eta = \frac{\dot{m}_c}{\dot{m}_M + \dot{m}_c} \quad (0 \leq \eta \leq 1) \quad (1)$$

was used to evaluate the sealing performance of each rim seal. The equation above can be transformed to

$$\eta = \frac{\phi - \phi_M}{\phi_C - \phi_M} \quad (2)$$

by considering continuity of CO_2 mass and thus can be directly calculated by measured CO_2 concentration.

Test Conditions

Test conditions were set similar to those of actual engine operations. Mainstream gas flow rate, cooling air flow rate and disk rotational speed were varied systematically so that non dimensional parameters representing each of the parameters above were varied in the region shown below.

Mainstream Reynolds number (representing mainstream flow)

$$1.1 \times 10^6 \leq Re_m \leq 2.4 \times 10^6 \quad (3)$$

Dimensionless flow coefficient (representing cooling air flow)

$$1.6 \times 10^3 \leq C_w \leq 1.3 \times 10^4 \quad (4)$$

Rotational Reynolds number (representing disk rotational speed)

$$1.6 \times 10^6 \leq Re_t \leq 3.0 \times 10^6 \quad (5)$$

Each parameter is defined as follows.

$$Re_m = \frac{V_{ax} b}{\nu_M} \quad (6)$$

$$C_w = \frac{Q_c}{\nu_c b} \quad (7)$$

$$Re_t = \frac{b^2 \omega}{\nu_c} \quad (8)$$

In experiments for the case with rotor blades, the combination of mainstream Reynolds number and rotational Reynolds number was set so that the rotor blade inlet relative velocity angle was similar to those of high-pressure turbine first stage rotor blades of actual engines.

NUMERICAL ANALYSIS

In order to get information about the flow structure in the rim seal and to establish a method to numerically predict seal effectiveness, unsteady CFD analyses were carried out.

The CFD program used for this study was UPACS (Yamane et al.) with modification to treat unsteady Rotor-Stator interactions. The UPACS solves three-dimensional time-accurate Reynolds Averaged Navier-Stokes (RANS) equations with zero or one-equation turbulence models. Baldwin-Lomax model was used in this study.

One of the most remarkable features of this program is its applicability to complicated geometries by means of multi-block

structured grid method. In the analyses presented here, the computational domain including not only the cavity but also the tip clearance area of vanes and blades was divided into multiple blocks. Parallel computation was performed on Numerical Simulator III (NS III) of Japan Aerospace Exploration Agency (JAXA).

Analyses were carried out for the pie-shaped domain shown in Fig.5. It included the cavity and the mainstream that covered one pitch of guide vane and rotor blade. This domain was divided into multiple blocks and structured grid was generated in each block.

As for boundary conditions, total pressure and total temperature measured in experiments were given at the inlet plane of the mainstream as well as at the inlet plane of the cooling air. At the exit plane static pressure was given. Cyclic conditions were given for cyclic boundary planes.

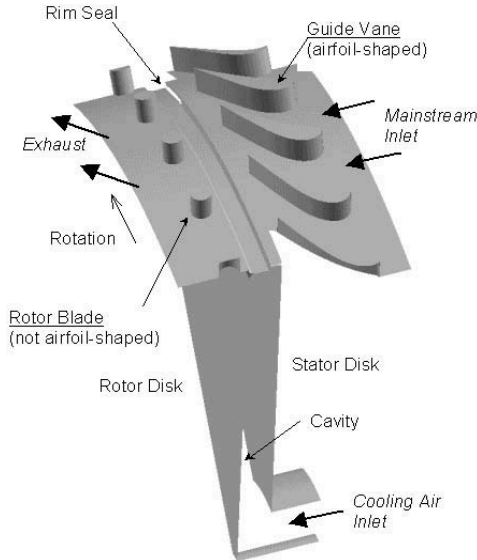


Fig.5 Computational domain

RESULTS AND DISCUSSIONS

Mainstream Static Pressure Distribution

Circumferential distribution of static pressure on the mainstream hub surface just downstream of the guide vanes is shown in Fig.6. Shown here is the distribution of static pressure normalized by dynamic pressure at the mainstream inlet.

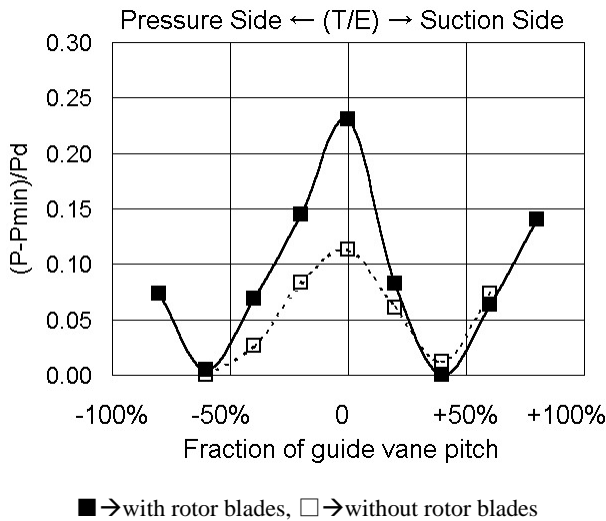


Fig.6 Static pressure distribution downstream of the guide vane (SEAL-1; $Re_m=2.4 \times 10^6$, $Re_t=3.0 \times 10^6$, $Cw=3.4 \times 10^6$)

As has been pointed out by preceding researchers, the static pressure asymmetry of the mainstream is considered to be the main driving force for mainstream gas ingestion. As for the downstream region of nozzles, the asymmetry is caused mainly by the wake of guide vanes. In addition, the presence of rotor blades located downstream has a significant influence on the static pressure distribution. In Fig.6, static pressure distribution for the case with rotor blades is larger than that for the case without rotor blades. This trend is considered to be consistent with the trend of measured seal effectiveness (seal effectiveness for the case with rotor blades is lower than that for the case without rotor blades) presented in the following section.

No significant circumferential distribution of static pressure could be seen in the cavity even if large mainstream flow generated a large circumferential distribution of static pressure in the mainstream.

Seal Effectiveness - Effect of Operating Conditions

Seal effectiveness measured at the outer region ($r/b=0.93$) on the stator disk surface under various operating conditions is shown in Fig.7(a) for the case without rotor blades and in Fig.7(b) for the case with rotor blades.

Compared with Case-1 (Case-4), seal effectiveness for Case-2 (Case-5) (smaller mainstream Reynolds number) tends to be significantly higher. This is considered to be because of smaller magnitude of static pressure asymmetry in the mainstream at downstream of the guide vanes.

Compared with Case-2 (Case-6), seal effectiveness for Case-3 (Case-4) (smaller rotational Reynolds number) tends to be slightly higher. This is considered to be because the inflow on the rotor disk surface, which compensates the outflow on the rotor disk surface driven by the pumping effect, is weak at lower rotational speed.

Although shown in Fig.7(a) and Fig.7(b) is only the data for SEAL-2, same qualitative trend was confirmed for SEAL-1.

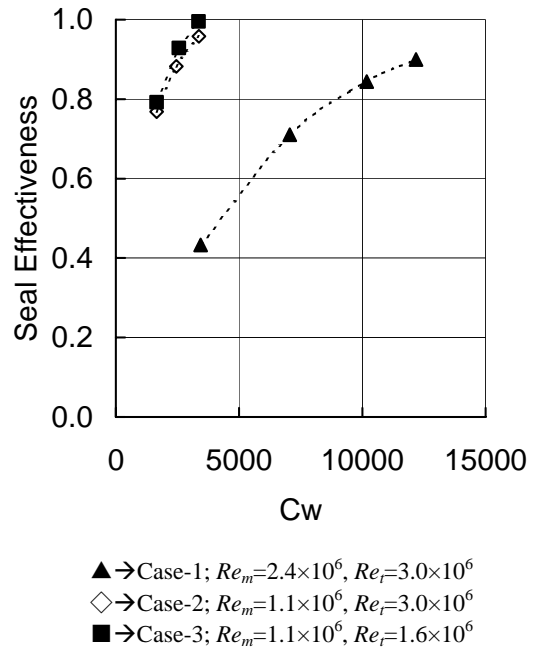
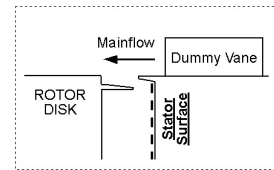


Fig.7(a) Effect of operating conditions on seal effectiveness (SEAL-2; at $r/b=0.93$; without rotor blades)

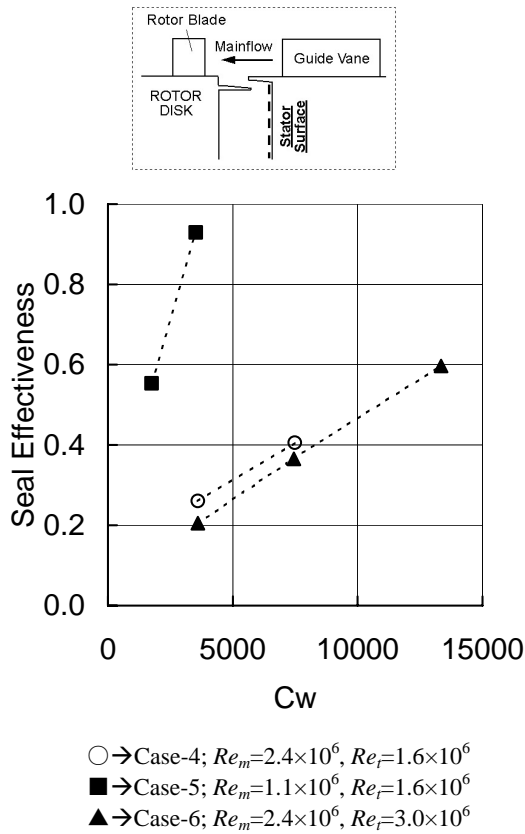


Fig.7(b) Effect of operating conditions on seal effectiveness (SEAL-2; at $r/b=0.93$; with rotor blades)

Seal Effectiveness - Effect of the Presence of Rotor Blades and Fin Overlap

Seal effectiveness measured for all configurations (i.e., both SEAL-1 and SEAL-2; both with and without rotor blades) is shown in Fig.8(a) for the outer region ($r/b=0.93$) and in Fig.8(b) for the inner region ($r/b=0.73$). Shown here are the data both on the stator surface and near the rotor surface.

The effect of the presence of rotor blades can be found by comparing the data for the case with and without rotor blades. For both SEAL-1 and SEAL-2, seal effectiveness for the case with rotor blades is lower than that for the case without rotor blades. This trend is significantly prominent on the stator surface at outer region of the cavity, whereas it is not clear near the rotor surface as well as at inner region ($r/b=0.73$) of the cavity (see Fig.8(b)). So it is clear that for the configurations examined here the presence of rotor blades degrades seal effectiveness. However the influence is limited to the stator surface at outer region of the cavity and the rotor surface whose temperature is critical to the structural integrity is less affected.

The effect of fin overlap can be found by comparing the data for SEAL-1 and SEAL-2. Unlike the effect of the presence of rotor blades, the effect of fin overlap shows adverse trend between the cases with and without rotor blades. For the case without rotor blades, seal effectiveness is higher for SEAL-2 (with overlap). On the other hand, for the case with rotor blades, seal effectiveness is higher for SEAL-1 (with gap). This trend, which is opposite to that expected, may be related to the mainstream static pressure distribution generated by the interference between the rotor blade upstream potential and the cooling air injected from the seal gap. As for SEAL-2, the cooling air is injected into the mainstream at the area close to the leading edge of rotor blades, which may generate more peaky distribution of static pressure resulting in more ingestion of mainstream gas.

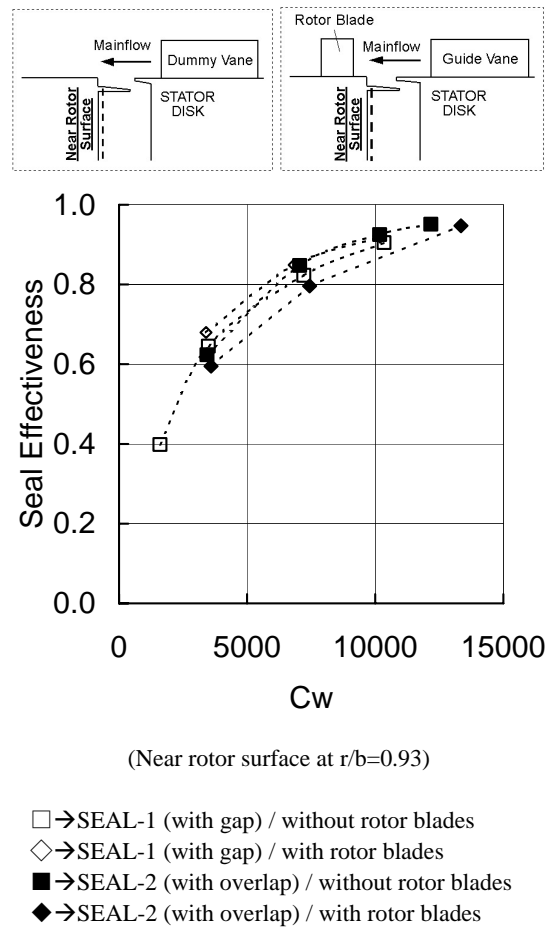
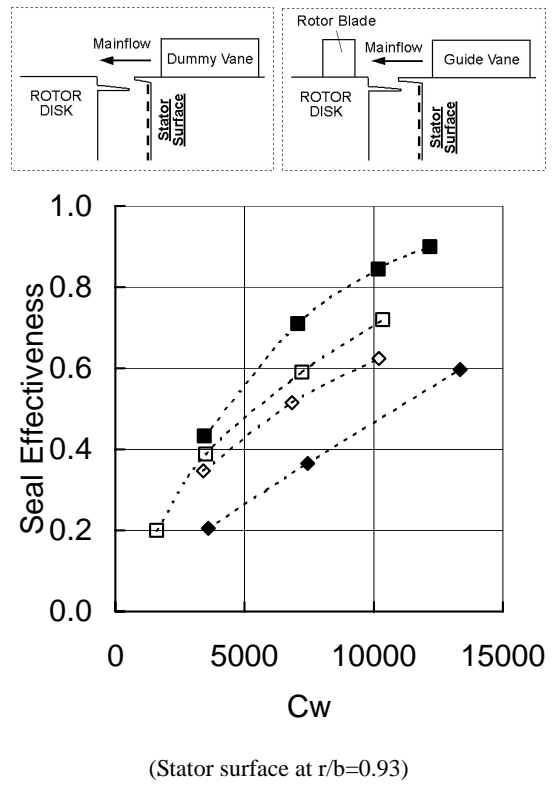
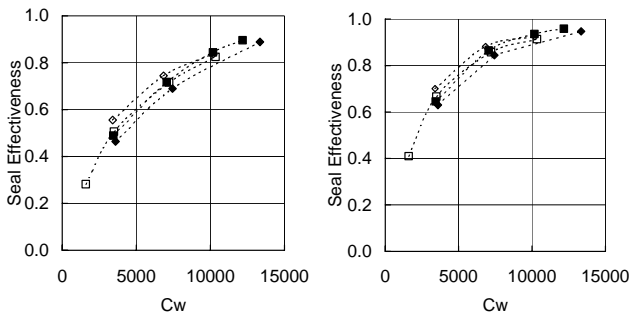


Fig.8(a) Effect of the presence of rotor blades and fin overlap on seal effectiveness at $r/b=0.93$ ($Re_m=2.4 \times 10^6$, $Re_r=3.0 \times 10^6$)



(Stator surface at $r/b=0.73$) (Near rotor surface at $r/b=0.73$)

Fig.8(b) Effect of the presence of rotor blades and fin overlap on seal effectiveness at $r/b=0.73$ ($Re_m=2.4 \times 10^6$, $Re_r=3.0 \times 10^6$)

Numerical Analysis Results

(1) Static Pressure Distribution in the mainstream

Static pressure distribution on the mainstream hub surface is shown in Fig.9. Shown here is the instantaneous distribution at the moment when the rotor blades locate at the mid pitch of the guide vanes.

Locally high-pressure zone can be seen upstream of the rotor blades as well as downstream of the guide vanes. The former is related to the upstream potential of the rotor blades and the latter to the wake of the guide vanes. The fact that the former high-pressure zone extends to the seal gap area supports the experimental results that the presence of the rotor blades degrades seal effectiveness, which was mentioned in the previous section.

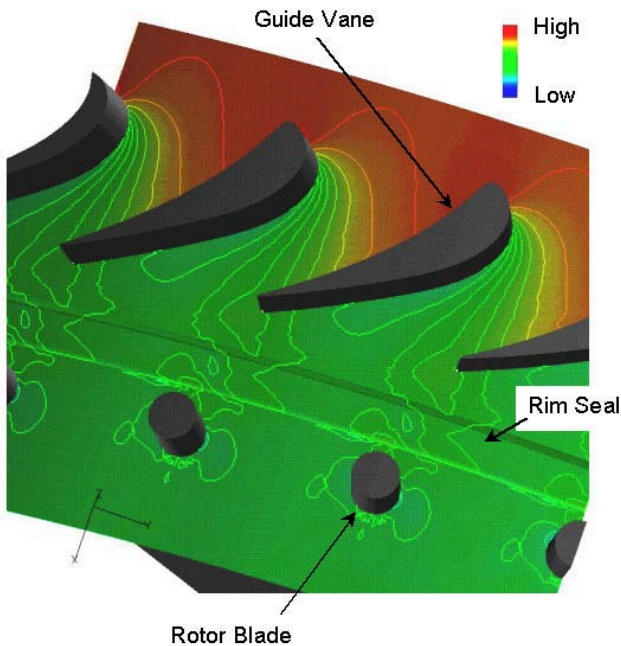


Fig.9 Static pressure distribution on the mainstream hub surface (SEAL-1; $Re_m=1.1 \times 10^6$, $Re_r=1.6 \times 10^6$, $Cw=3.3 \times 10^6$)

(2) Velocity Vector Plots inside the Rim Seal Area

Velocity vector plots in r-z section at five different circumferential positions representing one pitch of the guide vane are shown in Fig.10. The percentage value shown below each figure is the fraction of pitch. Positive value means that it is in the suction side. Presented here are the instantaneous plots at the

moment when the rotor blades locate at the same circumferential position as the guide vanes. In this figure vector plots incorporate only the radial and axial velocity components, so the large circumferential velocity component is not contained here.

The significantly varying flow pattern across one pitch of the guide vane is visible. Large inflow vectors showing the mainstream gas ingestion into the rim seal gap area can be seen from -40% to 0% of the pitch. As the rotor blades are presumed to locate in guide vane wakes at this moment, the strong inflow mentioned above might be generated by the rotor blade upstream potential effect. The mainstream gas ingested into the rim seal gap turns to the direction of the rotor rotation, flows on the rotor fin and finally ingests into the disk cavity at +20% of the pitch. The cooling air flow injected into the mainstream, for example at +40% of the pitch, may interfere with the rotor blade upstream potential and result in a peaky static pressure distribution, which cause more ingestion for the rim seal with overlap.

As mentioned above, the flow structure is significantly complicated and thus further investigations are needed to fully understand the flow structure.

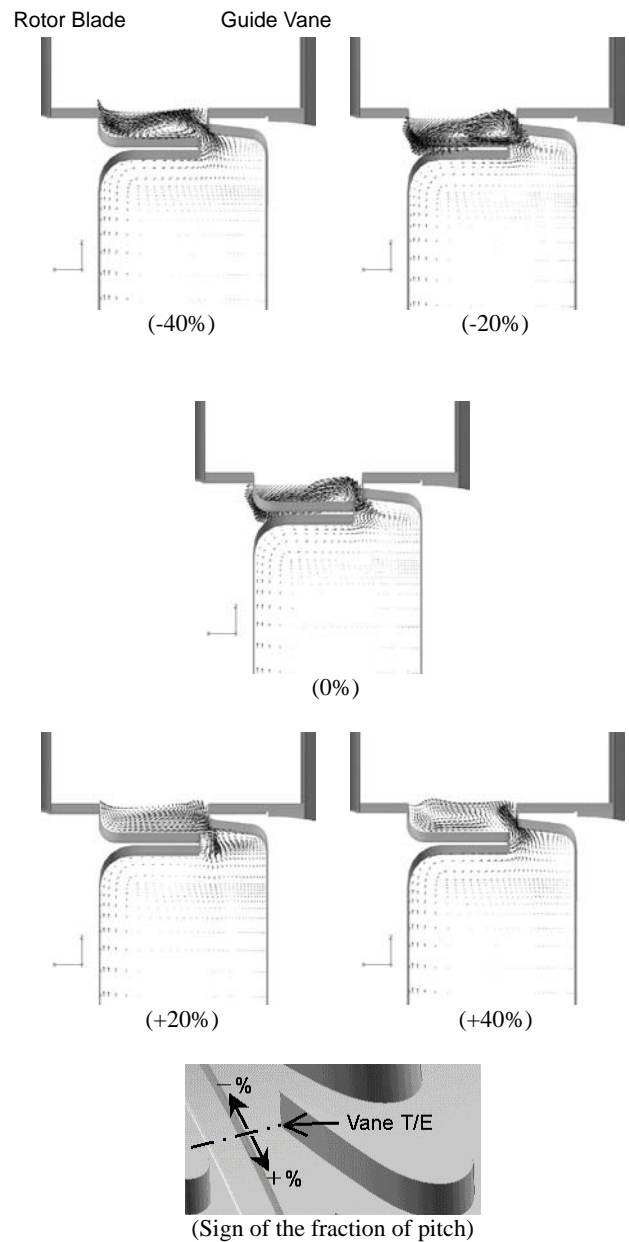


Fig.10 Velocity vector plots inside the rim seal (SEAL-1; $Re_m=1.1 \times 10^6$, $Re_r=1.6 \times 10^6$, $Cw=3.3 \times 10^6$)

CONCLUSIONS

Effectiveness of turbine rim seals in the cavity located upstream of the rotor disk was examined both experimentally and numerically.

- The effect of operating conditions (mainstream Reynolds number and rotational Reynolds number) on seal effectiveness was obtained, which was consistent in all configurations examined.
- It was shown that the presence of rotor blades degraded seal effectiveness whether there is an overlap or a gap. Especially, the influence was significant on the stator surface at outer region of the cavity and the rotor surface was less affected
- In case without rotor blades, seal effectiveness was higher for the rim seal with overlap. Meanwhile in case with rotor blades, seal effectiveness was higher for the rim seal with gap. This trend may be related to the mainstream static pressure distribution generated by the interference between rotor blade upstream potential and cooling air injected from the rim seal gap.
- Three-dimensional unsteady CFD analysis result showed that the velocity vector pattern varied significantly across one pitch of the guide vane. Further investigations are needed to fully understand the flow structure.

ACKNOWLEDGEMENTS

The authors would like to express thanks to the New Energy and Industrial Technology Development Organization (NEDO) and the Ministry of Economy, Trade and Industry (METI), who gave them the opportunity to conduct "Research and Development of Environmentally Compatible Propulsion System for New-Generation Supersonic Transport (ESPR) project". Numerical investigation was carried out by using UPACS on Numerical Simulator III (NS III) under joint research agreement between Japan Aerospace Exploration Agency (JAXA) and Ishikawajima-harima Heavy Industries Co., Ltd. (IHI). Cooperation of the persons involved in JAXA is gratefully acknowledged.

REFERENCES

- Abe, T., Kikuchi, J. and Takeuchi, H., 1979, "An investigation of turbine disc cooling," Paper GT30, 3rd CIMAC Congress, Vienna.
- Bayley, F. J. and Owen, J. M., 1970, "The fluid dynamics of a shrouded disk system with a radial outflow of coolant," *ASME Journal of Engineering for Gas Turbines and Power*, Vol. 92, pp.335-341.
- Bohn, D., Rudzinski, B., Sturken, N. and Gartner, W., 2000, "Experimental and Numerical Investigation of the Influence of Rotor Blades on Hot Gas Ingestion into the Upstream Cavity of an Axial Turbine Stage," ASME paper 2000-GT-284.
- Chew, J. W., Green, T. and Turner, A. B., 1994. "Rim sealing of rotor-stator wheelspaces in the presence of external flow," ASME paper 94-GT-126.
- Dadkhah, S., Turner, A. B., and Chew, J. W., 1991, "Performance of radial clearance rim seals in upstream and downstream wheelspaces," ASME paper 91-GT-32. (Also *ASME Journal of Turbomachinery*, Vol. 114, pp.439-445).
- Green, T., 1994, "Effect of external flow on sealing performance of rotor-stator rim seals," Ph.D. Thesis, University of Sussex, Sussex, UK.
- Green, T., and Turner, A. B., 1994, "Ingestion into the Upstream Wheel-space of an Axial Turbine Stage," *ASME Journal of Turbomachinery*, Vol. 116, pp.327-332.
- Hamabe, K. and Ishida, K., 1992, "Rim Seal Experiments and Analysis of a Rotor-Stator System with Nonaxisymmetric Main Flow," ASME Paper 92-GT-160.
- Hills, N. J., "Development and Application of Multigrid Methods in CFD for Turbine Rim Sealing," Ph.D. Thesis, University of Sussex, Sussex, UK.
- Hills, N. J., Green, T., Turner, A. B. and Chew, J. W., 1997,

"Aerodynamics of Turbine Rim-Seal Ingestion," ASME Paper 97-GT-268.

Phadke, U. P. and Owen, J. M., 1983, "An investigation of ingress for an air-cooled shrouded rotating disk system with radial clearance seals," *ASME Journal of Engineering for Gas Turbines and Power*, Vol.105, pp.178-183.

Roy, R. P., Xu, G. and Feng, J., 2000, "Study of Main-stream Gas Ingestion in a Rotor-Stator Disk Cavity," AIAA Paper 2000-3372.

Yamane, T., Yamamoto, K., Enomoto, S., Yamazaki, H., Takaki, R. and Iwamiya, T., "Development of a common cfd platform - UPACS -," in *Parallel Computational Fluid Dynamics -Proceedings of the Parallel CFD 2000 Conference Trondheim, Norway (May 22-25, 2000)*, pages 257-264. Elsevier Science B.V., February 2001.